JAAS

Accepted Manuscript

ROYAL SOCIETY OF CHEMISTRY

rsc.li/jaas

View Article Online
DOI: 10.1039/C8JA00055G

Quantitative elemental analysis of polymers through laser ablation - inductively coupled plasma by using a dried droplet calibration approach, DDCA

Ángela Villaseñor,[a] Marina Boccongelli[b] and José Luis Todolí[a]*

[a] Department of Analytical Chemistry, Nutrition and Food Sciences. University of Alicante, P. O. Box 99, 03080 Alicante, Spain.

E-mail: jose.todoli@ua.es

[b]Total Research & Technology Feluy, Zone Industrielle C, B-7181 Feluy, Belgium

View Article Online
DOI: 10.1039/C8JA00055G

The so called Dried Droplet Calibration Approach (DDCA) was applied for the first time to the determination of elemental concentration in polyethylene and polypropylene samples by means of inductively coupled plasma optical emission spectrometry (ICP-OES) and mass spectrometry (ICP-MS). Based on this novel calibration strategy, small volumes (*c.a.*, 1 μL) of a series of multielemental aqueous standard solutions were deposited on the sample solid surface. Afterwards, the droplets were dried and a significant fraction of the remaining solid residues (*i.e.*, 80% of their surface area) was ablated. The integrated signals were plotted against the mass of added analyte ablated per laser shot. The analyte concentration in the sample was obtained by extrapolation of the obtained calibration lines. A study demonstrating the existence of matrix effects was carried out and it was noticed that carbon was not an appropriate internal standard because it did not compensate for changes in the absolute amount of ablated material as a function of the sample matrix. In contrast, elements such as Sc and Y mitigated this effect. External calibration using a polymeric support also proved to be inefficient from the point of view of accuracy. In contrast, the DDCA presented as an outstanding feature the compensation for matrix effects, because with this method both sample and added standard were simultaneously ablated and the generated aerosols reached the plasma together. The accuracy of the DDCA was demonstrated by means of the analysis of three polymer certified reference materials. It was verified that, in general terms, there were not significant differences between the elemental certified concentrations and those obtained by applying the DDCA. Furthermore, three polyethylene and three polypropylene samples were analyzed following both the DDCA and a reference method based on their acid digestion and further ICP analysis. Both methodologies provided similar results for Al, Ti, Si, Cr, Ca, Zn and Mg. For

View Article Online
DOI: 10.1039/C8JA00055G

elements either potentially volatile or present at low concentrations, such as As, Hg and Ti in some polymers, there were significant discrepancies between certified and measured values.

1. Introduction

Additives are usually incorporated to polymers in order to modify specific material properties such as flame and UV resistance, color or elasticity. Among these additives, metals and metalloids play a very important role and their content and distribution may influence the polymers behavior.[1,2,3,4,5,6]

Nevertheless, an important number of regulations must be complied because some elements can be harmful to consumers and/or the environment. Therefore, there is a growing interest in developing analytical methods to carry out elemental analysis of polymers. Secondary ion mass spectrometry (SIMS), auger electron spectroscopy (AES) and micro X-ray fluorescence spectroscopy (μ-XRF)[7] are suitable techniques to analyze solid surfaces. However, SIMS and AES suffer from strong matrix effects and need ultrahigh vacuum conditions. Besides, these techniques have limitations in terms of attainable depth (<5 μm). Meanwhile, limits of detection achieved by μ-XRF are usually high.[8] Glow discharge optical emission or mass spectrometry (GD-OES/MS) offer high depth resolution (10 nm). Besides, the atomization and ionization processes are separated in space and time thus giving rise to a mitigation of matrix effects and, hence, quantification without the absolute need for matrix-matched calibration standards is possible. However, this technique shows

View Article Online
DOI: 10.1039/C8JA00055G

restricted lateral resolution (on the order of mm) and requires certain conditions related with the vacuum level, the sample shape and its dimensions.[9]

Nowadays, elemental analysis of polymers can be carried out using spectroscopic techniques such as inductively coupled plasma optical emission spectroscopy (ICP-OES) or mass spectrometry (ICP-MS). Unfortunately, in most of the cases lengthy dissolution protocols must be applied, that may cause sample contamination and losses of volatile components.[10,11]

Laser ablation (LA) coupled to ICP-OES or ICP-MS allows the direct determination of additives in polymers with minimal or no sample preparation.[1,2,10,12] However, severe matrix and fractionation effects may be observed when working with nanosecond pulsed lasers. [1,13] Although femtosecond lasers are promising devices,[14] several methods have been proposed to mitigate these phenomena as, for instance, an external calibration using solid certified reference materials as standards.[11,15,16,17] Unfortunately, the sample ablation yield depends strongly on the type of polymer and, hence, it is still difficult to find suitable solid standards.[10,18,19]

In order to compensate for changes in the sample ablated mass as a function of the matrix, [20] an element acting as internal standard (IS) can be selected.[20,21[Carbon has been suggested as a good candidate because of its known concentration in polymers and its uniform distribution within the samples. [4,10,22] Furthermore, it has been observed that there is a virtually linear correlation between the carbon ablated mass and the ICP signal whose slope is independent of the polymer type [4]. However, the applicability of C as internal standard has been in dispute over the years because the laser beam causes polymer pyrolysis. Therefore, unlike the analytes, carbon is

View Article Online
DOI: 10.1039/C8JA00055G

transported to the plasma in both gaseous and particulate phases thus giving rise to a differentiated signal behaviour.[11,22,23]

Kumtabtim *et al.*,[24] applied external calibration for urine analysis. Sample droplets were deposited on solid substrates such as paper, glass slide and Teflon sheet. An infrared lamp was used to eliminate the solvent and the residue left was analyzed through LA-ICP-MS. Matrix matched synthetic standards enriched with the analytes of interest were prepared and also deposited on the supports. Later, Resano *et al.*[25,26] performed the analysis of liquid biological samples according to the so called dried matrix spots (DMS).[27] Samples such as blood (DBS, dried blood spots)[28] or urine (DUS, dried urine spots) as well as standards were separately deposited on a filter paper, dried and subsequently analyzed through LA-ICP-MS. A similar calibration method was proposed for the analysis of biological solid samples by LA-ICP-MS.[29,30] Voss *et al.*[6] applied a strategy based on the deposition of standards on porous nylon disks to the analysis of polymers. However, the discrepancies observed between measured and expected concentrations could be attributed to differences between the interaction of the laser beam with nylon and the polymer samples.

A novel calibration method termed dried droplet calibration approach (DDCA) was suggested for the analysis of solid samples through LA-ICP-MS.[31] Small volumes of aqueous standards were deposited at different locations on the sample surface. The dry solid residues obtained after droplet evaporation were ablated together with the solid sample. Therefore, the analyte contained in both the solid deposit and the sample contributed to the ICP signal finally obtained. The feasibility of this method for quantitative LA-ICP-MS analysis was demonstrated by analyzing a glass certified reference material and fused beads containing a fraction of refining catalysts .

View Article Online
DOI: 10.1039/C8JA00055G

The aim of the present work was thus to apply the new calibration method, for the first time, to the analysis of polymers by means of LA-ICP-OES and LA-ICP-MS. Besides, the DDCA was combined with internal standardization using C, Sc and Y as reference elements. The reliability of the method was verified in two different ways: *(i)* analyzing three polyethylene reference materials; and, *(ii)* comparing the results obtained using the DDCA against those provided by a classical method based on sample acid dissolution and further ICP analysis of the digests. Another goal of the present work was to demonstrate the capability of the DDCA as a straightforward method allowing the analysis of polymers having different composition and structure such as polyethylene and polypropylene.

2. Experimental

2.1. Chemicals and samples

Standards were prepared from an ICP 1,000 mg L^{-1} multielemental (Merck IV, Merck KGaA, Darmstadt, Germany) and Ti, Si, Br, Sb and Hg 1,000 mg L^{-1} single element stock solutions (Merck). The corresponding solutions were prepared in ultrapure water (R < 18.2 MΩ cm) obtained from a Mili-Q system (El Paso, TX, USA). In order to visualize the solid deposits on the sample surface, 100 mg L^{-1} of methylene blue were added to the standards. The results suggested that the presence of this coloring agent did not have any influence on the ICP signal.

An automatic pipette (Eppendorf, Hamburg, Germany) was used to deposit 1.000 ± 0.025 µL of the standards on the polymer surface. The droplets were

View Article Online
DOI: 10.1039/C8JA00055G

subsequently evaporated until dryness by inserting the samples in an oven at 40 ^{o}C for 45 minutes.

Three polyethylene certified reference materials (BCR 681, BCR 680K and BCR 680) were analyzed to evaluate the precision and accuracy of the DDCA. Table 1 summarizes the certified elemental concentrations. Besides, three polypropylene (#1, #2 and #3) and three polyethylene (#4, #5 and #6) samples were analyzed by applying the DDCA. A conventional acid digestion method was taken as reference. The sample treatment was carried out in a microwave oven (Start D, Milestone, Soriole, Italy). The samples were cut and ground and 0.25 g ±0.1 mg were inserted into a Teflon vessel containing 10 mL of nitric acid. The reactors were sealed and introduced into the oven at 200 ^{o}C for 15 min. Afterward, a 30 min cooling step was applied. The volume of the obtained solutions was made up to 25 mL with ultrapure water in graduated flasks. After each sample digestion, the reactors were cleaned by applying 30 min microwave cycles with nitric acid. Finally, elemental concentration was determined through ICP-OES using standards with nitric acid matched concentration.

2.2. Instrumentation

A Nd:YAG solid state laser ablation system LSX-213 G2+ (CETAC, Omaha, USA) operated at 213 nm under Q-switched mode was used throughout. The LA chamber was equipped with an ablation cup to remove quickly the aerosol from the sample surface. Three gas streams were used; helium 1 carried the aerosol out of the ablation chamber whereas helium 2, together with an argon stream, delivered the particles leaving the ablation cell to the plasma through a 40 cm length transfer tube.

View Article Online
DOI: 10.1039/C8JA00055G

The laser ablation system was coupled to either a 7700X Agilent ICP-MS spectrometer (Agilent, Santa Clara, USA), to determine trace elements, or a Perkin Elmer 4300DV system ICP-OES (Uberlingen, Germany) when polymers contained elements at high enough concentrations. Table 2 summarizes the operating conditions. The ICP-MS spectrometer was used in the collision cell mode with helium.

A Hitachi S-3000N Scanning Electron Microscope (SEM) was used to characterize the shape and dimensions of the line scans and craters obtained on the different tested samples.

3. Results and discussion

3.1. Development of the proposed calibration methodology

The DDCA involved the determination of the sample ablated mass per pulse. The polymer surface was first cleaned[32] and 20 mm diameter, 2 mm thickness sample disks were weighed with a closed Mettler Toledo micro-balance (precision of ± 1 µg). After ablation with a known number of laser shots the sample disks were weighed again in order to determine the mass of sample ablated (M_S) as the difference between the initial and the final weight. The number of pulses required to achieve a measurable weight difference with a good precision depended on the sample analyzed. For example, in the case of polyethylene, 120,000 laser shots were required to ablate 3 mg of sample. This procedure provided RSDs values (n=5) lower than 5%. Besides, the total number of pulses, N_p, was calculated according to:

View Article Online
DOI: 10.1039/C8JA00055G

$$N_p = \frac{\sum_{N_r} L_r}{V_s} f \qquad (1)$$

where N_r was the number of selected line scans, L_r the length of each one of the line scans, *f* the shot frequency and V_s the scan rate.

Therefore, the sample ablated mass per pulse, M_p, was given by the following equation:

$$M_p = \frac{M_S}{N_p} \qquad (2)$$

Note that the sample could be weighed before and after the analysis to measure M_s. A series of droplets corresponding to aqueous multielemental standards were deposited on the sample surface and subsequently dried giving rise to round-shaped residues with diameters close to 2 mm. The mass of analyte ablated from each solid residue, m_A, was calculated by applying:

$$m_A = C\ V\ S_A \qquad (3)$$

where C was the analyte concentration in the aqueous standard, V the volume of the droplet deposited on the solid sample (*i.e.*, 1 µL) and S_A the percentage the solid residue surface area that was actually ablated. It was experimentally verified that from 5 to 6 minutes were required to ablate the entire deposit. S_A in equation (3) was obtained from the laser beam diameter (Ø), the length of each particular line scan (L_r), the number of line scans used to ablate the dried droplets (N_r), the distance between line scans (S_L) and the length of the non-ablated sample surface (L_w):

$$S_A = \frac{ablated\ area}{total\ residue\ area} = \frac{\sum_{N_r} L_r \cdot \phi}{\sum_{N_r} L_r \cdot \phi + \sum_{N_r - 1} L_w \cdot S_L} 100 \qquad (4)$$

View Article Online
DOI: 10.1039/C8JA00055G

The width of the line scan, measured by SEM was in good agreement with the laser beam diameter chosen, *i.e.*, 150 µm for polyethylene samples. In contrast, in the case of polypropylene, the experimentally determined diameter of the line scan was higher (170 µm) than the nominal one. A possible explanation was based on the shielding effect caused by the confined plasma.[2221] This phenomenon was promoted by the high number of pulses on a given sample area, i.e., 120 pulses. Besides, it is generally accepted that samples with weak UV absorption, as for example polypropylene, show higher penetration depths, resulting in bigger ablation craters.[10] Once m_A was calculated, it was divided by N_p thus giving rise to the independent variable in the calibration lines.

In the DDCA method both, the standard and the sample, were continuously and simultaneously ablated and the generated aerosols were mixed in the ablation cell and transfer tube. The calibration line was obtained by plotting the sum of intensities obtained for each solid residue (n=3) versus m_A/N_p (*i.e.*, the mass of added analyte that was actually ablated from each solid residue per laser pulse). The analyte mass originally contained in the sample ablated per pulse (m_s) was determined by extrapolation of the calibration line (Figure 1.a). An increase in the m_A/N_p value induced a grow in the integrated signal that could be adjusted to a linear model. The plot of the residuals revealed that they were distributed between positive and negative values (Figure 1.b) giving support to the selected model. Regarding the correlation coefficient, R^2 was comprised between 0.9917 and 0.9999 depending on the analyte and the sample. The errors of the slope (s_b) and the intercept (s_a) for the example considered in Figure 1 were 1.5×10^9 and 1.6×10^6, respectively. These values represented a 5.0 and 16 % of the respective slope and intercept values. Finally, the

View Article Online
DOI: 10.1039/C8JA00055G

covariance, S_{xy}, was estimated and it was verified that positive values of this magnitude were always obtained. For instance, for Figure 1, S_{xy} took a value close to 1.3 x 10^4, thus revealing a good positive correlation between the integrated intensity and the analyte ablated mass per laser pulse.[33]

Once the mass of analyte and sample ablated per pulse were known, it was possible to determine the analyte concentration in the polymer (C_A^S):

$$C_A^S = \frac{m_s}{M_p} \qquad (5)$$

It is worth mentioning that the analyte spatial distribution within the solid residues was not homogeneous. Figure 2.a plots the two dimensional distribution of the aluminum emission intensity for a solid residue deposited on a polyethylene. It was noticed that this analyte was preferentially located in the outermost area of the solid residue. A completely different elemental distribution was observed when the droplet was deposited on a different polyethylene (Figure 2.b). In the case of a polypropylene sample (Figure 2.c), aluminum was more homogeneously distributed. Therefore, the spatial distribution of the analytes in the solid residues depended on the particular substrate. Consequently, a significant surface (75-85%) of the solid residues had to be ablated. Note that, the elemental spatial distribution on a given deposit, was the same regardless of the analyte considered.

The use of ethanol as a solvent was also evaluated. Ethanol has a lower surface tension and viscosity than water and, hence, the droplet was more spread on the polymer surface. It was experimentally observed that, provided that the analytes were distributed in a large sample surface area, there was a higher number of signal spikes within the solid residues than when using water as solvent. Besides, the large residue

View Article Online
DOI: 10.1039/C8JA00055G

area increased the time required to fully ablate it. As a result, water was used as the solvent throughout the present study.

3.2. Optimization of the laser operating conditions

The optimization of the laser operating conditions was carried out in terms of ICP-OES sensitivity for two different polymers: polyethylene and polypropylene. As it has been discussed in previous studies,[34] the laser energy influenced the sample ablated mass. It was confirmed that the sensitivity grew with the laser energy until this parameter reached a value of 2.25 mJ. Taking into account the laser beam diameter (200 µm), this corresponded to a fluence of 7.15 J cm^{-2}. Above this level, the variations in signal were virtually negligible[35] likely because the ablation products absorbed or scattered a fraction of the laser beam energy.[36] Besides, the plasma shielding produced on the sample surface was also intensified.[40] An additional explanation was based on changes in the ablation mechanism, *i.e.*, from non-thermal to thermal, when the fluency reached high values.[37] It is worth mentioning that, at fluencies much higher than the ablation threshold, re-deposition of large debris around the crater could lead to fractionation effects.[38,39,47] The laser fluence was finally kept at 7.94 J cm^{-2} because this value was above the ablation threshold for both polyethylene and polypropylene while minimized thermal effects.

The laser beam diameter, in turn, was kept at its maximum value, *i.e.*, 200 µm, in order to shorten the analysis time and to compensate for eventual sample

View Article Online
DOI: 10.1039/C8JA00055G

heterogeneities. As regards the shot frequency, it was found that the higher the laser repetition rate the higher the sensitivity regardless of the matrix considered. Therefore, this variable was kept at 20 Hz. The laser scan rate, also affecting the analysis time and the sample ablation efficiency, was set at 25 µm s^{-1} because it was verified that, under these conditions, a single scan line was sufficient to completely ablate the totality of the residue. Regarding the He and Ar flow rates, the best results in terms of ICP-OES signal corresponded to 0.3, 0.1 and 0.1 L min^{-1} for helium 1, helium 2 and argon streams, respectively. Meanwhile, for ICP-MS the respective flow rates providing maximum sensitivities were: 0.5, 0.3 and 0.3 L min^{-1}.

3.3. Effect of the solid residue on the sample ablation yield

Two droplets with 0 and 50 mg L^{-1} analyte concentrations were deposited on several polymers and the carbon emission signals were measured in presence and in absence of solid residue. For some samples, both sets of signals were not significantly different regardless the added analyte concentrations. Thus, for instance, in the case of polyethylene #6, the carbon signal when ablating the deposit generated from a 0 mg L^{-1} droplet was similar to that for the clean polymer. For Polypropylene #2, carbon signal was not affected by the presence of the residue resulting from a 50 mg L^{-1} multielemental standard. Finally, the carbon signals found when ablating the residues on polyethylene #5 were independent of the analyte mass deposited. Other polymers (*i.e.*, polyethylene #4) afforded signals with significant non-systematic variations as a function of the analyte concentration in the deposited standards.

View Article Online
DOI: 10.1039/C8JA00055G

Therefore, it was concluded that the variations observed in C signals, were due neither to the presence of solid residues nor to the deposited analyte mass.

Similar trends were found for analytes. For instance, for an element present in the polymer (*e.g.*, Si) it was concluded that there were no differences between signals corresponding to the clean polymers and those originating from a 50 mg L^{-1} solid residue that did not contain Si. A possible explanation could be based on the number of pulses received by a given sample location (*c.a.,* 160 pulses for 200 μm laser diameter, 25 μm s^{-1} sample displacement speed and 20 Hz laser shot frequency). Note that the sample was continuously in movement and, hence, a portion of fresh residue was simultaneously ablated together with the polymer beneath. Furthermore, taking into account the detection conditions of the spectrometers (see Table 2), it was estimated that every signal point was the result of 20 and 50 laser pulses in ICP-OES and ICP-MS, respectively.

In order to illustrate the mixing efficiency between the standard and the sample in the ablation cell and/or transport line, the signals for Si (*i.e.*, present in the sample but not included in the multielemental standard) were compared against those for Ti (*i.e.*, only present in the standard). It was experimentally verified that both, the intensity and the signal stability, remained unaltered when the laser switched from the clean polymer to the polymer spiked with the solid deposit (Figure 3). Therefore, it was concluded that the aerosols generated from the sample and standard arrived simultaneously to the plasma.

3.4. Repeatability

View Article Online
DOI: 10.1039/C8JA00055G

With regard to the repeatability of the DDCA methodology, seven droplets of a 20 mg L^{-1} multielemental standard solution were deposited at different locations on polypropylene #3. Table 3 summarizes the RSD values corresponding to the mean integrated intensities of the seven solid residues. It was clearly observed that, in order to achieve good precisions (RSD < 10%), the residues should be completely ablated.

3.5. Influence of the matrix composition

Before applying the new DDCA, the sample ablated mass per pulse, M_p, was determined for all the polymers studied. Five replicates were done with RSD values lower than 5%. The influence of the matrix composition on the ablation yield was clearly evidenced. It is interesting to note that M_p was virtually the same for all the polypropylene samples (from 31 to 35 ng $pulse^{-1}$). However, in the case of polyethylene, M_p significantly differed from low density (22 ng $pulse^{-1}$) to reference (29 ng $pulse^{-1}$) samples. Both the CRM 680 and CRM 681 were high density polyethylene (HDPE) samples while the CRM 680 K was a low density one. Therefore, the discrepancies in terms of M_p were likely due to changes in the efficiency of light absorption by the different polymers at the laser wavelength. In fact, the certified reference polymers were green whereas the rest of polyethylene samples were white. These results anticipated a dependence of the signal on the polymer nature.

The influence of the sample matrix on the ablation process was further studied by examining the craters generated by SEM. Figure 4 shows two representative examples obtained on a high density polyethylene (#8) and a polypropylene (#3). Several observations suggested the polymer melting induced by the laser: *(i)* in the

View Article Online
DOI: 10.1039/C8JA00055G

case of polyethylene (Figure 3.a) filaments appeared around the crater; *(ii)* in marked contrast, a significant amount of spherical particles were deposited at the crater sourroundings when the polypropylene sample was under study (Figure 3.b); and, *(iii)* for polyethylene, the microcavities initially generated on the crater walls disappeared as increasing the number of pulses.[40] Expectedly, the characteristics of the craters depended on the polymer (Figure 4). Finally, the aerosol characterization, supported the conclusion that, besides fusion, polymers undergone thermal degradation, thus giving rise to gaseous carbon containing compounds.[41,42]

An additional study was carried out to verify the existence of matrix effects. Droplets of a given aqueous standard (20 μg mL^{-1}) were deposited on six different polymers. Figure 5 reveals that the integrated intensities for polypropylene #1 and #3 were higher than those obtained for polyethylene samples (#4 and #5). This result was in full agreement with M_p. Co and Mn were not present in the polymers studied and, thus, their signals originated exclusively from the residue. In order to try to explain the observed trend, the ICP-OES argon signal was monitored and it was verified that the polymer nature did not modify it significantly. Therefore, it appeared that a high polymer ablation yield favored the transport of the analyte contained in the deposits.

However, although the three polypropylene samples provided the same ablation mass per laser shot, the integrated intensity in case of polypropylene #2 was lower than those obtained for the rest of polypropylene samples. In fact, it was similar to that observed for the polyethylene #5. As a conclusion, the type of polymer affected severely the ablation process. A method such as the DDCA, could compensate for all these effects, because a calibration line was generated from every particular sample.

View Article Online
DOI: 10.1039/C8JA00055G

3.6 Internal standard

The use of IS is relatively common both in ICP-OES and ICP-MS.[43,44,45,46] Therefore, an additional investigation using C as internal standard was carried out. Besides, 20 μg mL^{-1} yttrium and scandium were added to all the standard solutions to correct for volume variations of the deposited droplets.

After normalization of the Co and Mn intensities to the carbon ones (Figure 6), it was clearly noticed that both ratios varied as a function of the polymer tested. This suggested that the selection of carbon as internal standard was not appropriate to correct for matrix effects in polymers. It should be considered that, unlike Co or Mn, carbon was partially delivered to the plasma in vapor phase. [22] Furthermore, carbon has a high first ionization potential (11.3 eV) and, hence, its intensity may be affected by slight changes in plasma thermal conditions that do not necessarily affect in the same extent the analytical signals.[11] In previous reports it has been claimed that there is a linear relationship between carbon ablated mass and signal regardless the polymer structure.[4] This trend was also observed in the present work. Nonetheless, this fact did not imply that carbon was a good internal standard, because, as mentioned before (Figure 5), for a given analyte concentration, the signal depended strongly on the polymer structure. Furthermore, a plotting of carbon signal versus time gave rise to a signal recording with lower fluctuations (RSD = 1.5%, n =30) than the situation found for the analytes (RSD = 9.1, n=30).

A condition that must be fulfilled by an element in order to be considered as an efficient IS is that its behavior all along the system should be the same as that for the analyte. Therefore, the effect of a given matrix on the ablation yield, analyte transport

View Article Online
DOI: 10.1039/C8JA00055G

efficiency and plasma processes must be similar for both the analyte and the IS. [15,22,23,47,48,49] During the ablation event, carbon is partially transformed into vapour whereas the analytes are not. Therefore, the transport efficiency is expected to be much higher for the former element. Finally, the performance of carbon in the plasma is completely different as compared to an analyte arriving in solid phase. [22,23,42,50] Thus, processes such as the analyte vaporization and atomization could cause a delay in the analyte excitation and/or ionization. All these comments could explain why carbon did not compensate for eventual changes in analytical signal induced by the matrix nature (Figure 6).

The presence of carbon in the plasma has proven to cause ICP-MS space charge effects and charge transfer reactions. [51,52] However, it should be stated that, according to the DDCA procedure, the amount of carbon introduced into the plasma was virtually identical for samples and standards.

When the Mn and Co signals were normalized to the scandium and yttrium signal intensities (Figure 7), the corresponding ratios were less dependent on the matrix, although for the high-density polyethylene #6 the ratio was significantly lower than for the remaining samples.

3.7. External calibration

External calibration based on the deposition of reference solutions on a porous nylon disk has been recently proposed for reliable polymers analysis. [6] In this work, droplets from aqueous standard solutions containing increasing elemental concentrations were deposited on a polystyrene support. It is important to consider

View Article Online
DOI: 10.1039/C8JA00055G

that the mass of polystyrene ablated (12 ng pulse^{-1}) was much lower than those for both polypropylene and polyethylene (35 and 20 ng pulse^{-1}, respectively). Therefore, a correction factor was used to compensate for these differences.

Interestingly, in the case of polyethylene, the analyte concentrations obtained for magnesium, titanium, and zinc i.e., 1285±189, 1.8±1.0, 59±11 mg Kg^{-1}, respectively, were in good agreement with those obtained by microwave acid digestion i.e., 1005±98, 1.9±0.3, 53±2 mg Kg^{-1}, respectively. However, the results for aluminum and calcium depended on the method assayed. For the polypropylene sample, magnesium, calcium, aluminum and titanium, provided discrepancies between methods. Therefore, it was concluded that the external calibration strategy using a polystyrene support did not provide good results.

An additional investigation was performed using similar polymers. Thus, the support chosen for the dried droplets reference solutions had the same matrix as the sample. Polyethylene #6 was used as a support to analyze polyethylene #4. The analytical concentrations obtained were different from those expected. This was in agreement with the results previously reported, as the discrepancies observed among polyethylene samples (Figure 5) were not removed even with the use of internal standards.

3.8. Accuracy of the calibration methodology

Once it was demonstrated that the polymer matrix had a significant effect on the ablation efficiency and that this phenomenon could not be alleviated by means of external calibration or IS, the new calibration methodology was applied to the analysis

View Article Online
DOI: 10.1039/C8JA00055G

of three certified reference materials (BCR 681, BCR 680 K and BCR 680). Table 4 compares the elemental concentrations obtained using the DDCA with the certified values.

In order to compare the results provided by the DDCA with the certified ones, statistical tests were carried out considering the values of the concentrations and their uncertainties. [53]

$$U_{\Delta} = 2u_{\Delta} \Rightarrow u_{\Delta} = \sqrt{u_m^2 + u_{CRM}^2} \qquad (6)$$

where u_m is the uncertainty of the measurement result, u_{CRM} the uncertainty of the certified value and u_{Δ} the combined uncertainty of the result experimentally obtained and certified value. U_{Δ} was compared with the absolute difference between the measured and certified concentration ($\triangle_m$).

In the case of the BCR 681, only for As and Hg the measured concentrations were higher than the certified values, although for As the difference between the measured and certified concentration was rather low (Table 4). The concentrations of the rest of elements were not different from the certified ones according to the U_{Δ} and $\triangle_m$ values. When considering the BCR 680K CRM, the measured mean values were not significantly different from the certified ones ($U_{\Delta} \geq \triangle_m$). Only slight discrepancies between the measured concentrations and the certified ones were observed for As, and Br. The deviations observed for As and Hg in both BCR 680K and BCR 681 could be assigned to the low concentration of these elements in the certified reference materials. Besides, the high volatility of species containing these elements could explain why experimentally obtained Hg and As concentrations were higher than the

View Article Online
DOI: 10.1039/C8JA00055G

certified ones. Further investigations would be required to discern the chemical form of these elements in polymer CRMs.

When analyzing the BCR 680, the measured concentrations for all the elements were not significantly different from the certified values ($U_\Delta > \triangle_m$). Br was not determined in this sample because of its extremely high content.

View Article Online
DOI: 10.1039/C8JA00055G

3.9. Analysis of polymer samples

The dried droplet calibration approach was also applied, for the first time, to the analysis of six polymers. Tables 5 and 6 summarize the concentrations obtained using this new calibration strategy together with those provided by the polymer acid digestion procedure.

According to F and t tests, there were not statistically significant differences between the concentrations afforded by both methods with a probability of 95% (α=0.05) (t calculated for the different elements= 0-2.3, t tabulated= 2.776). Only for titanium contained in both polypropylene #1 and polyethylene #4 and chromium found in polyethylene #4, the obtained concentrations by the new DDCA were differed from those given by the microwave digestion method. These discrepancies could be assigned to the low concentration of these elements in the polymers. Besides, the concentration for Zn in polyethylene #4 was higher than the expected one.

Conclusions

Changes in the polymer structure, causing differences in absorption of UV light and thermal properties as glass transition temperature or melting temperature, cause matrix effects when carrying out elemental analysis by means of laser ablation – ICP-OES and ICP-MS. These phenomena are difficultly eliminated by using external calibration or internal standardization. Regarding the latter method, carbon cannot be efficiently used as IS although additional elements such as Sc or Y could mitigate these matrix effects.

View Article Online
DOI: 10.1039/C8JA00055G

A straightforward calibration method such as that described in the present work is a useful strategy to compensate for matrix effects. With the dried droplet calibration approach, DDCA, a calibration line is obtained for every particular sample. Therefore, the proposed method avoids complex schemes such as matrix matching or selection of an appropriate CRM for each polymer.

Taking into account conventional digestion methods, the DDCA avoids the problems related with contamination and increases the sample throughput. Thus, a complete analysis of ten samples took about 3 and 5 h for the DDCA and the microwave digestion, respectively. Furthermore, unlike the latter method, the former one, did not require from sample dilution what led to a sensitivity high enough to perform elemental analysis of polymer samples.

The DDCA shows good precision and accuracy and has been successfully applied, for the first time, to the analysis of nine different polymer samples. Additional studies are required to apply such as method to the localized polymer samples. These experiments are currently being developed in our laboratories and will be the subject of future reports.

View Article Online
DOI: 10.1039/C8JA00055G

References

1. M. Hemmerlin, J.M. Mermet, *Spectrochim. Acta, Part B,* 1996*,* **51,** 579-589.
2. T. Stehrer, J. Heitz, J.D. Pedarnig, N. Huber, B. Aeschlimann, D. Günther, H. Scherndl, T. Linsmeyer, H. Wolfmeir, E. Arenholz, *Anal. Bioanal. Chem*., 2010, **398**, 415-424
3. L. Kempenaers, N.H. Bings, T.E. Jeffries, B. Vekemans, K. Janssens, *J. Anal. At. Spectrom.,* 2001, **16**, 1006-1011.
4. D. Deiting, F. Borno, S. Hanning, M. Kreyenschmidt, T. Seidl, M. Otto*, J. Anal. At. Spectrom*., 2016, **31**, 1605-1611.
5. A.M.Dobney, A.J.G. Mank, K.H. Grobecker, P.Conneely, C.G. de Koster, *Anal. Chim. Acta*, 2000, **423**, 9-19.
6. M. Voss, M.A.G. Nunes, G.Corazza, E.M.M. Flores, E.I.Müller, V.L.Dressler, *Talanta,* 2017, **170**, 488-495.
7. B. Beckhoff, B. Kanngießer, N. Langhoff, R. Wedell, H. Wolff (Eds.), Handbook of Practical X-Ray Fluorescence Analysis, Springer, 2006.
8. B. Kanngiegera, W. Malzer, A. Fuentes-Rodriguez, Ina Reiche, *Spectrochim. Acta, Part B*, 2005, **60**, 41 – 47.
9. J. Pisonero and D. Günther, *Mass Spectrom. Rev.,* 2008, **27**, 609-623.
10. D. Deiting, F. Börno, S. Hanning, M. Kreyenschmidt, T. Seidl, M. Otto, *J. Anal. At. Spectrom*., 2016, **31**, 1605.

View Article Online
DOI: 10.1039/C8JA00055G

11. M. Resano, E. García-Ruiz, F. Vanhaecke, *Spectrochim. Acta, Part B* 2005, **60**, 1472-1481.

12. M. Hemmerlin and J.M. Mermet, *Spectrochim. Acta, Part B,* 1997, **52**, 1687-1694.

13 . R. E. Russo, X. Mao, H. Liu, J. Gonzalez, S. S. Mao, *Talanta*, 2002, **57**, 425–51.

14. D. Günther, B. Hattendorf, *Trends Anal. Chem.*, 2005, **24**, 255-265.

15. N. Miliszkiewicz, S. Wales, A. Tobiasz, *J. Anal. At. Spectrom*., 2015, **30**, 327-338.

16. M.E. Shaheen, J.E. Gagnon, B.J. Fryer, A. Polat, *Int. J. Mass Spectrom.*, 2017, **421**, 104-115.

17. A. Sajnóg, A. Hanc, R. Koczorowski, D.Baralkiewicz, *Talanta,* 2017, **175**, 370-381.

18. F.O. Leme, Q. Godoi, P.H.M. Kiyataka, D. Santos Jr, J.A.M. Agnelli, F.J. Krug, *Appl. Surf. Sci*, 2012, **258**, 3598-3603.

19. T. Stehrer, J. Heitz, J. D. Pedarnig, N. Huber, B. Aeschlimann, D. Günther, H. Scherndl, T. Linsmeyer, H. Wolfmeir and E. Arenholz, *Anal. Bioanal. Chem.*, 2010, **398**, 415–424.

20. J. Pisonero, B. Fernández and D. Günther, *J. Anal. At. Spectrom*., 2009, **24**, 1145-1160.

21. J. Koch and D. Günther, *Applied Spectroscopy*, 2011, **65**, 155A-162A.

22. D.A. Frick and D. Günther, *J. Anal. At. Spectrom*., 2012, **27**, 1294-1303.

23. A. Limbeck, P. Galler, M. Bonta, G. Bauer, W. Nischkauer, F. Vanhaecke, *Anal. Bioanal. Chem.,* 2015, **407**, 6593-6617.

24. U. Kuntabtim, A. Siripinyanond, C. Auray-Blais, A. Nywari, J.S. Becker, *Int. J. Mass Spectrom.*, 2011, **307**, 174-181.

View Article Online
DOI: 10.1039/C8JA00055G

25. M. Armendía, L. Rello, F. Vanhaecke, M. Resano, *Anal. Chem.*, 2012, **84**, 8682-8690.

26. M. Resano, M. Aramendía, L. Rello, M. L. Calvo, S. Bérail, C. Pécheyran, *J. Anal. At. Spectrom.*, 2013, **28**, 98–106.

27. M. Resano, M. A. Belarra, E. García-Ruiz, M. Aramendía, L. Rello, *Trends Anal. Chem.*, 2018, **99**, 75–87.

28. M. Aramendía, L. Rello, S. Bérail, A. Donnard, C. Pécheyran, M. Resano, *J. Anal. At. Spectrom.,* 2015, **30**, 296-309.

29. M.A.G. Nunes, M. Voss, G. Corazza, E. M.M. Flores, V.L.Dressler*, Anal. Chim. Acta*., 2016, **905**, 51-57.

30. M. Bonta, B. Hegedus, A. Limbeck, *Anal. Chim. Acta*., 2016, **908**, 54-62.

31. A. Villaseñor, C. Greatti, M. Boccongelli, J.L. Todolí, *J. Anal. At. Spectrom.*, 2017, **32**, 587.

32. D. Pietroy, Y. Di Maio, B. Moine, E. Baubeau, E. Audouard, *Opt. Express*, **20**, 2012, 29900—29908.

33. Massart, D. L.; Vandeginste, B. M. G.; Buydens, L. M. C.; De Jong, S.; Lewi,P. J.; Smeyers-Verbeke, X. X. Handbook of Chemometrics and Qualimetrics Part A; Elsevier: Amsterdam, 1997.

34. R.E. Russo, X. Mao, J.J. Gonzalez, V. Zorba, J. Yoo, *Anal. Chem*., 2013, **85**, 6162-6177

35. P. R. D. Mason, A. J. G. Mank, *J. Anal. At. Spectrom.*, 2001, **16**, 1381–1388.

36. A. A. Serafetinides, C. D. Skordoulis, M. I. Makropoulou and A. K. Kar, *Appl. Surf. Sci.*, 1998, **135**, 276–284.

View Article Online
DOI: 10.1039/C8JA00055G

37. M. E. Shaheen, B. J. Fryer, *Laser Part. Beams*, 2012, **30**, 473–479.

38. M. E. Shaheen, J. E. Gagnon, B. J. Fryer, *J. Appl. Phys.*, 2013, **114**, 83110.

39. T. Hirata, R. W. Nesbitt, *Geochim. Cosmochim. Acta*, 1995, **59**, 2491-2500.

40. Z.Q.Liu, Y.Feng, X.S. Yi., *Appl. Surf. Sci.*, 2000, **165**, 303-308.

41. J.L. Todolí, J.M. Mermet, *Spectrochim. Acta, Part B*, 1998, **53**, 1645-1656.

42. J.L. Todolí, J.M. Mermet, Polymer analysis and degradation, New York, Nova Science Publishers, Inc., 2000, ch.15.

43. F. Vanhaecke, H. Vanhoe, R. Dams, *Talanta*, 1992, **39,** 737-742.

44. C. Agatemor, D. Beauchemin, *Anal. Chim. Acta*, 2011, **706**, 66-83.

45. X. Romero, E. Poussel, J.M. Mermet, *Spectrochim. Acta, Part B,* 1997, **52**, 487-493.

46. J.W. Olesik, *Anal.Chem.* 1991, **63,** 12-21 A.

47. H.P. Longerich, D. Günther, S.E. Jackson, *J. Anal. Chem*, 1996, **335,** 538-542.

48. S. Zhang, M. He, Z. Yin, E. Zhu, W. Hang, B. Huang, *J. Anal. At. Spectrom.*, 2016, **31**, 358-382.

49. D. W. Hahn, N. Omenetto, *Appl. Spectrosc.,* 2012*,* **66***,* 347-419.

50. D.A. Frick, C. Giesen, T. Hemmerle, B. Bodenmiller, D. Günther, *J. Anal. At. Spectrom,* 2015, **30,** 254-259.

51. A.S. Al-Ammar, E. Reitznerova, R.M. Barnes, *Spectrochim. Acta, Part B*, 1999, **54**, 1813-1820.

52. D. Fliegel, C.Frei, G.Fontaine, Z.Hu, S. Gao, D. Günther, *Analyst*, 2011, **136**, 4925-4934.

53. T. Linsinger, ERM Application Note 1, European Commission-Joint Research Centre, Institute for Reference Materials and Measurements (IRMM), 2010.

View Article Online
DOI: 10.1039/C8JA00055G

Table 1. Certified reference materials and elemental concentrations.

Element	Concentration (mg Kg^{-1})		
	BCR 681 (High density polyethylene)	BCR 680K (Low density polyethylene)	BCR 680 (High density polyethylene)
As	3.93 ± 0.15	4.1 ± 0.5	30.9 ± 0.7
Br	98 ± 5	96 ± 4	808 ± 19
Cd	21.7 ± 0.7	19.6 ± 1.4	141 ± 2
Hg	4.50 ± 0.15	4.64 ± 0.2	25 ± 1
Pb	13.8 ± 0.7	13.6 ± 0.5	108 ± 3
Sb	-	10.1 ± 1.6	-

View Article Online
DOI: 10.1039/C8JA00055G

Table 2. Optimized operating conditions

Ablation system	
Ablation frequency/ Hz	20
Spot size/ µm	200
Scan rate/ µm s^{-1}	25
Pulse energy	2.7 mJ $pulse^{-1}$
Gas flow rates He / L min^{-1}	0.5 and 0.3 (ICP-MS)
	0.3 and 0.1 (ICP-OES)
ICP-MS system	
RF power/ KW	1.55
Carrier gas/ L min^{-1} (Ar added to the aerosol leaving the ablation cell)	0.3
Cell Collision (He)/ mL min^{-1}	3.0

View Article Online
DOI: 10.1039/C8JA00055G

Isotopes measured	^{52}Cr, ^{75}As, ^{81}Br, ^{111}Cd, ^{121}Sb, ^{202}Hg, ^{208}Pb
Plasma gas flow rate/ L min^{-1}	15.0
Auxiliar gas flow rate/ L min^{-1}	0.9
Integration time/mass s^{-1}	0.1
Sampling depth/ mm	5
ICP-OES system	
RF power/ KW	1.35
Carrier gas/ L min^{-1}	0.1
View Distance/ mm	15
Plasma viewing mode	Axial

View Article Online
DOI: 10.1039/C8JA00055G

Elements, wavelength/ nm	Al 396.152, C 193.090, Ca 317.933, Ca 315.887, Cd 214.438, Co 238.346, Cr 267.716, Li 670.784, Mg 280.270, Mn 257.610, Pb 220.353, Sc 357.635, Si 212.412, Sr 407.771, Ti 334.904, Ti 336.121, Y 371.030, Zn 213.856
Plasma gas flow rate/ L min^{-1}	15.0
Auxiliary gas flow rate/ L min^{-1}	0.2
Integration time/ ms	100
Read time/ s	1

Table 3. Relative standard deviations (RSDs) of the ICP-OES integrated signals obtained for different residues ablated areas.

View Article Online
DOI: 10.1039/C8JA00055G

Element	% Ablated residue surface area		
	100	60-70	20-30
Mg	2.9	7.2	13.8
Zn	6.9	10.3	15.5
Mn	7.3	12.6	16.1
Pb	9.2	13.4	20.7
Cd	10.4	11.9	16.0
Co	7.8	12.4	15.2
Sr	10.1	10.9	23.2
Li	6.3	8.4	12.5
Ca	7.9	8.3	10.6
Al	4.88	10.78	7.99

View Article Online
DOI: 10.1039/C8JA00055G

Table 4. Comparison of the certified concentrations with those obtained in ICP-MS by the new dried droplet calibration approach for three CRMs.

Element	BCR 681 (mg Kg^{-1})		BCR 680 K (mg Kg^{-1})		BCR 680 (mg Kg^{-1})	
	DCCA	Certified	DCCA	Certified	DCCA	Certified
As	6.2 ± 0.5	3.93 ± 0.15	7.0 ± 1.3	4.1 ± 0.5	30 ± 7	30.9 ± 0.7
Br	94 ± 12	98 ± 5	113 ± 7	96 ± 4	-	808 ± 19
Cd	21 ± 8	21.7 ± 0.7	16 ± 5	19.6 ± 1.4	137 ± 45	140.8 ± 2.5
Cr	21 ± 3	17.1 ± 0.6	21 ± 3	20.2 ± 1.1	117 ± 12	114.6 ± 2.6
Hg	22 ± 11	4.50 ± 0.15			25 ± 12	25.3 ± 1.0
Pb	14 ± 3	13.8 ± 0.7	15 ± 2	13.6 ± 0.5	106 ± 3	107.6 ± 2.8
Sb			11.5 ± 1.4	10.1 ± 1.6		

View Article Online
DOI: 10.1039/C8JA00055G

Table 5. Comparison of the concentrations (mg Kg^{-1}) obtained by the new dried droplet calibration in ICP-OES method and those calculated after microwave digestion of the three polypropylene samples.

Element	PP1		PP2		PP3	
	DCCA	Digestion	DCCA	Digestion	DCCA	RRT
Al	30 ± 3	29 ± 2	42 ± 4	40 ± 2	61 ± 6	50 ± 6
Ca	28 ± 3	28 ± 3*	50 ± 5	49 ± 5*	40 ± 4	34 ± 2
Mg	7 ± 2	6.4 ± 0.3			59 ± 19	58 ± 7
Ti	1.40 ±0.17	0.39 ± 0.08			-	1.1 ± 0.3
Zn	-	-			6.3 ± 0.5	4 ± 2

*The RSD associated to these values was 10%.

View Article Online
DOI: 10.1039/C8JA00055G

Table 6. Comparison of the concentrations (mg Kg^{-1}) obtained by the new dried droplet calibration in ICP-OES method and those calculated after microwave digestion of the three polyethylene samples.

	PE4		PE5		PE6	
Element	DCCA	Digestion	DCCA	Digestion	DCCA	Digestion
Al	37 ± 10	47 ± 8			346 ± 101	334 ± 60
Ti	0.33 ± 0.06	1.9 ± 0.3	6.1 ± 1.1	6.0 ± 0.2		
Si	-	-	-	117 ±6		
Cr	-	-	1.92 ±0.17	2.39 ±0.04	-	
Ca	6 ± 3	3 ± 2				
Zn	126 ± 7	53 ± 2				
Mg	1166 ± 296	1005 ± 98				

View Article Online
DOI: 10.1039/C8JA00055G

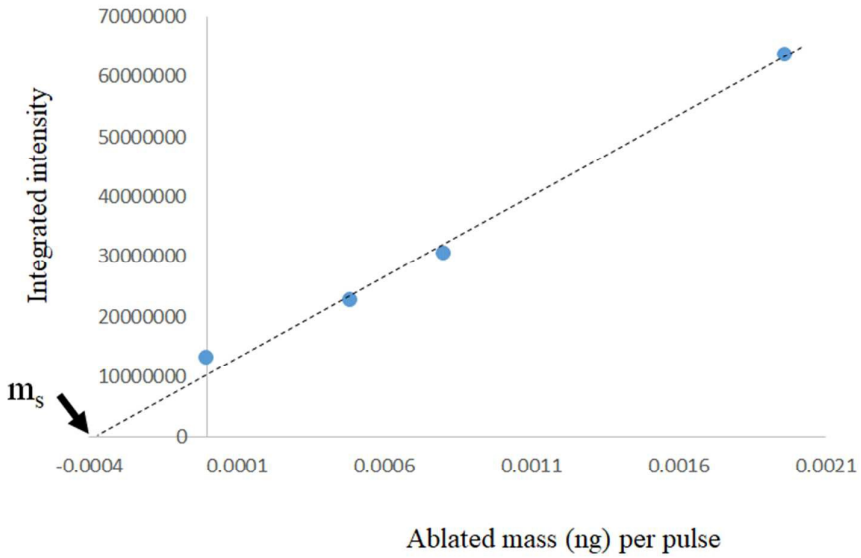

(a)

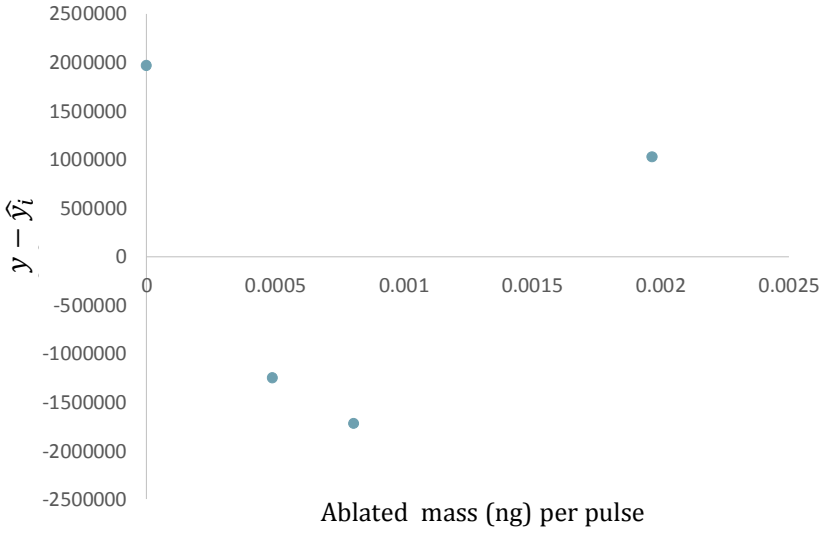

(b)

Figure 1. Calibration line (a) and residuals plotting (b) obtained for polyethylene # 8 in ICP-MS. Element: Pb.

View Article Online
DOI: 10.1039/C8JA00055G

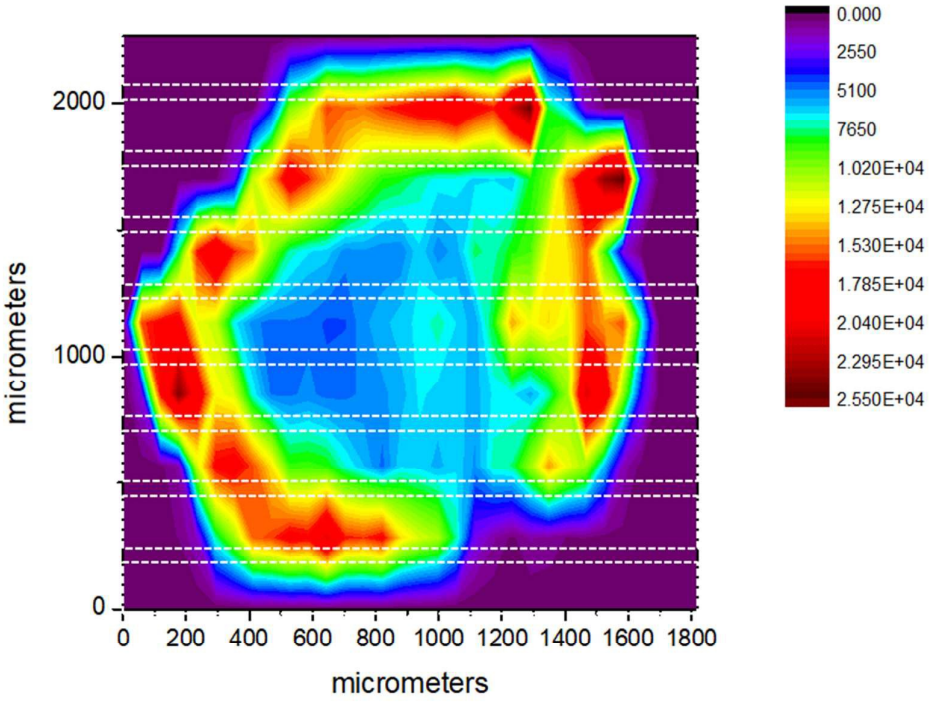

(a)

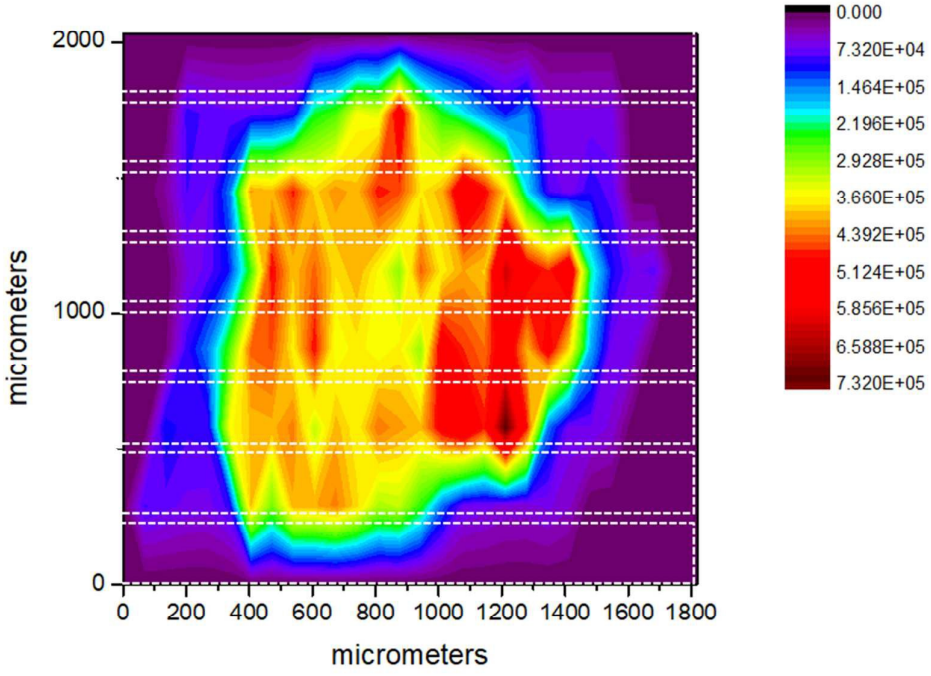

View Article Online
DOI: 10.1039/C8JA00055G

(b)

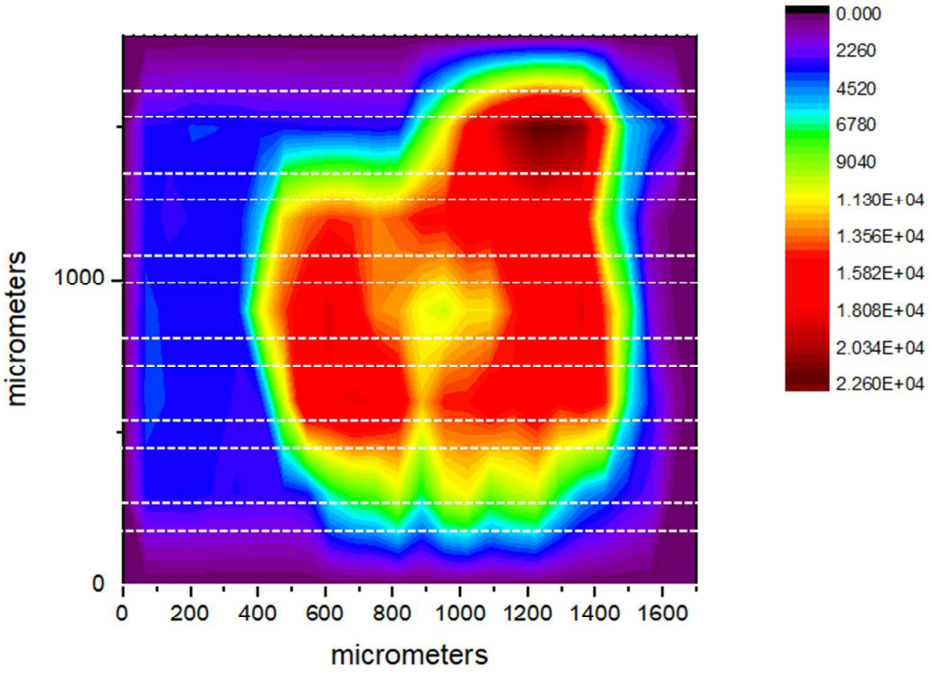

(c)

Figure 2. Spatial distribution of ICP-OES aluminum emission intensity corresponding to the solid residue deposited on three polymers. (a) polyethylene #5; (b) polyethylene #7; (c) polypropylene #1. Aluminum concentration in the aqueous standard: 20 μg mL^{-1}.

View Article Online
DOI: 10.1039/C8JA00055G

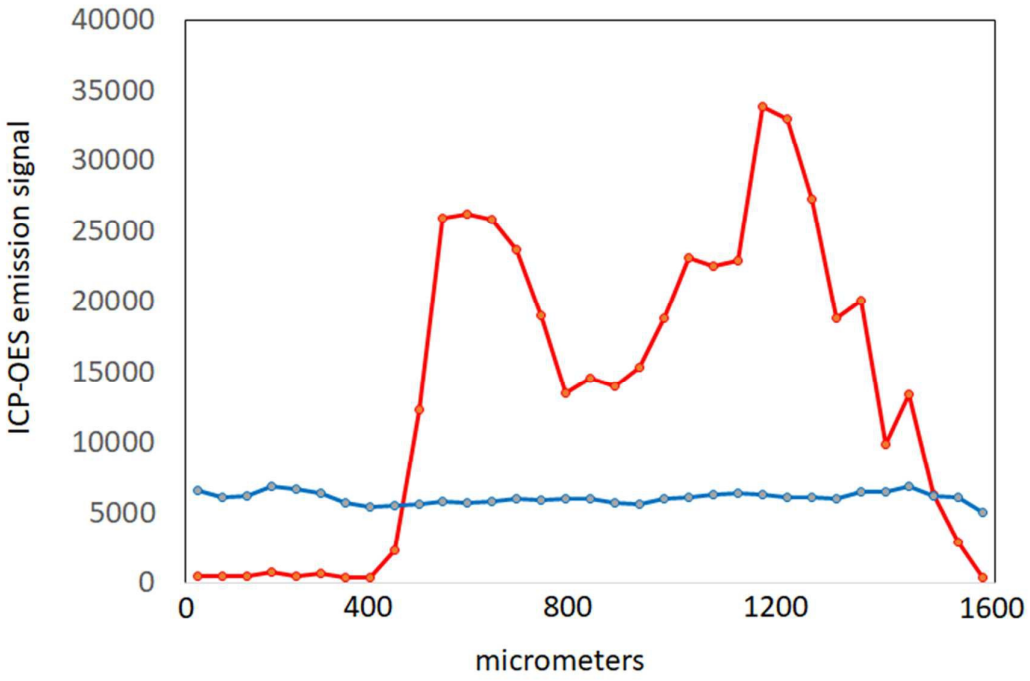

Figure 3. ICP-OES emission signal versus lateral position for polypropylene #2. Red line: Ti (element only present in the added standard, 20 μg mL^{-1}); blue line: Si (element only present in the sample). Note that each point was the result of 20 laser shots.

View Article Online
DOI: 10.1039/C8JA00055G

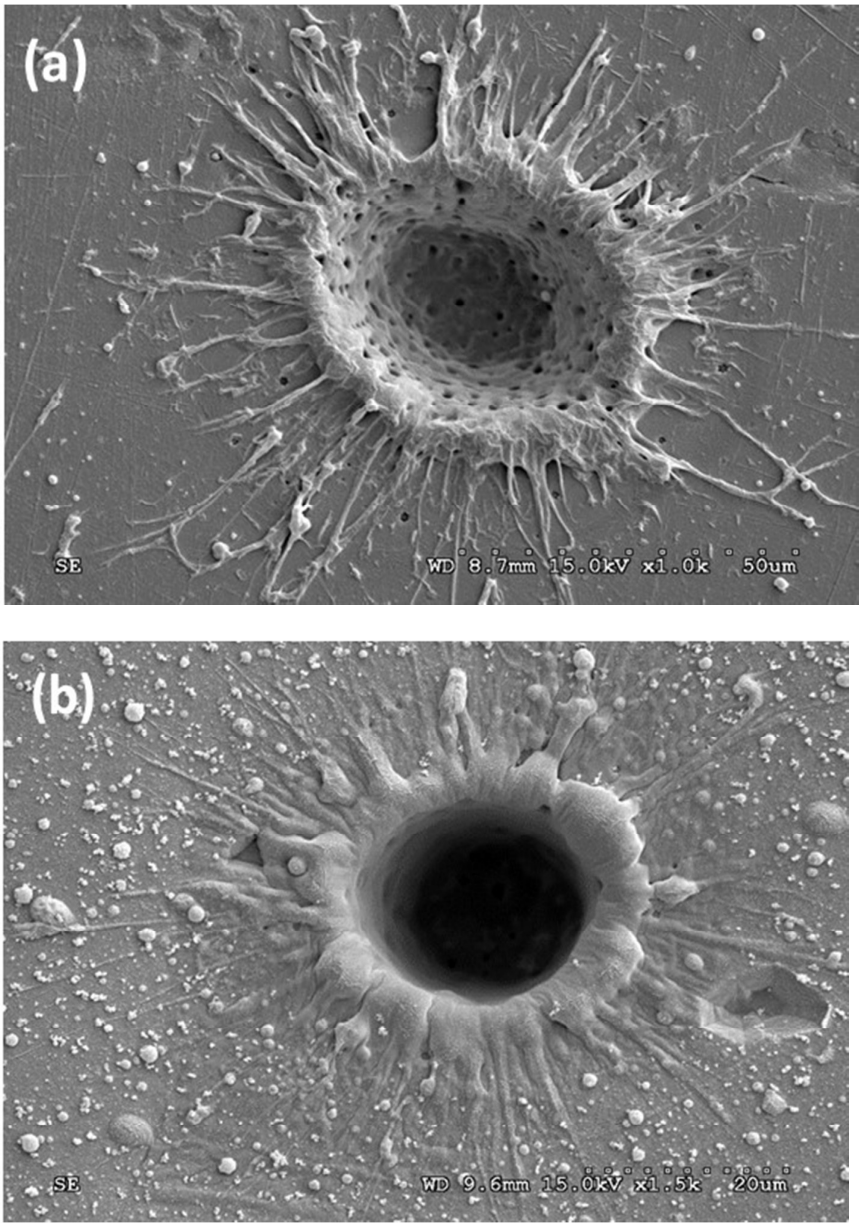

Figure 4. SEM images corresponding to the craters generated on the surface of (a) polyethylene #4 and (b) polypropylene #1. Laser beam diameter: 20 μm; pulse frequency: 20 Hz; laser shots: 20; pulse energy: 2.7 mJ.

View Article Online
DOI: 10.1039/C8JA00055G

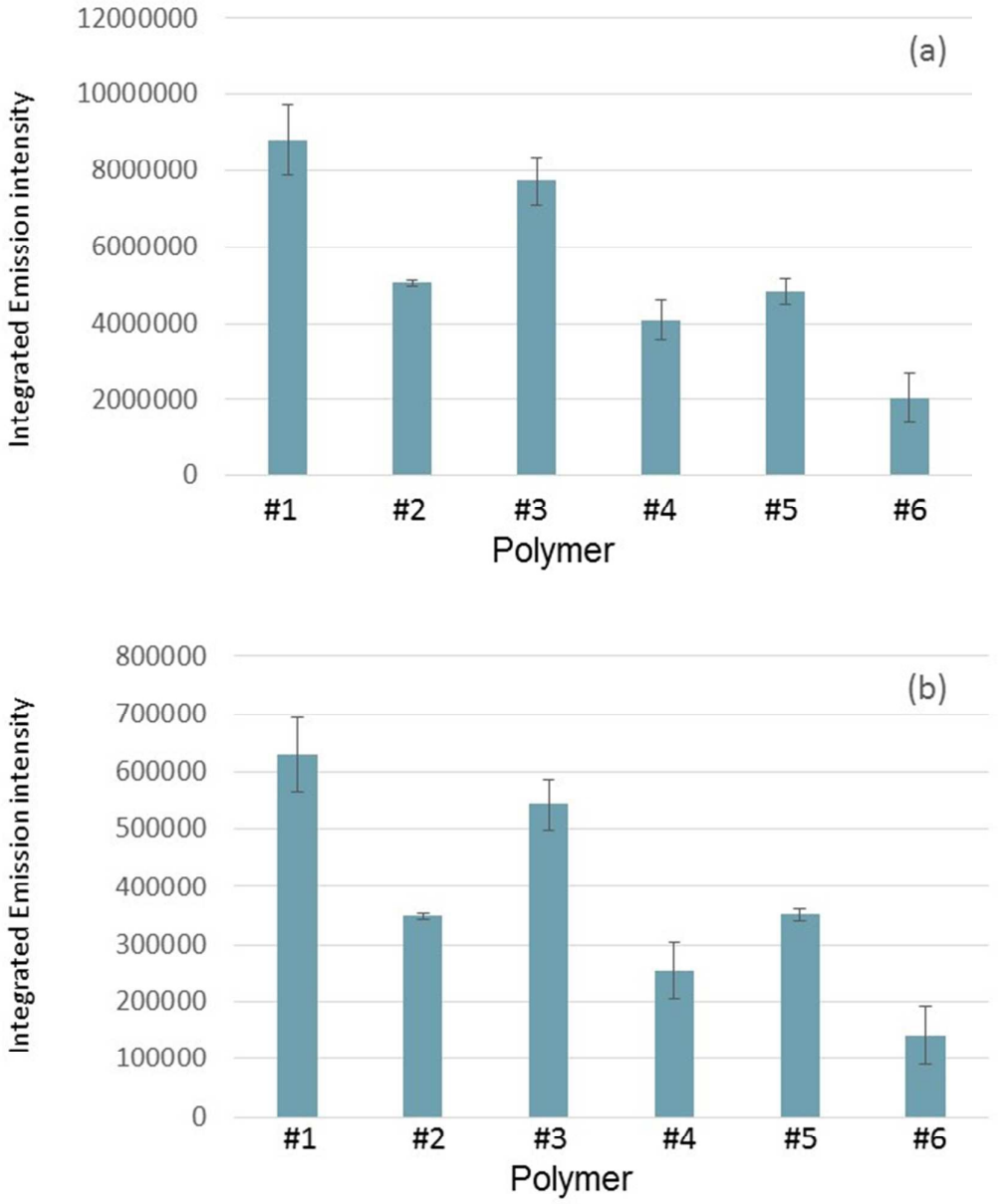

Figure 5. ICP-OES integrated emission intensity for the residues on six different polymers. (a) Manganese; (b) cobalt. Analytes concentration: 20 μg mL^{-1}.

View Article Online
DOI: 10.1039/C8JA00055G

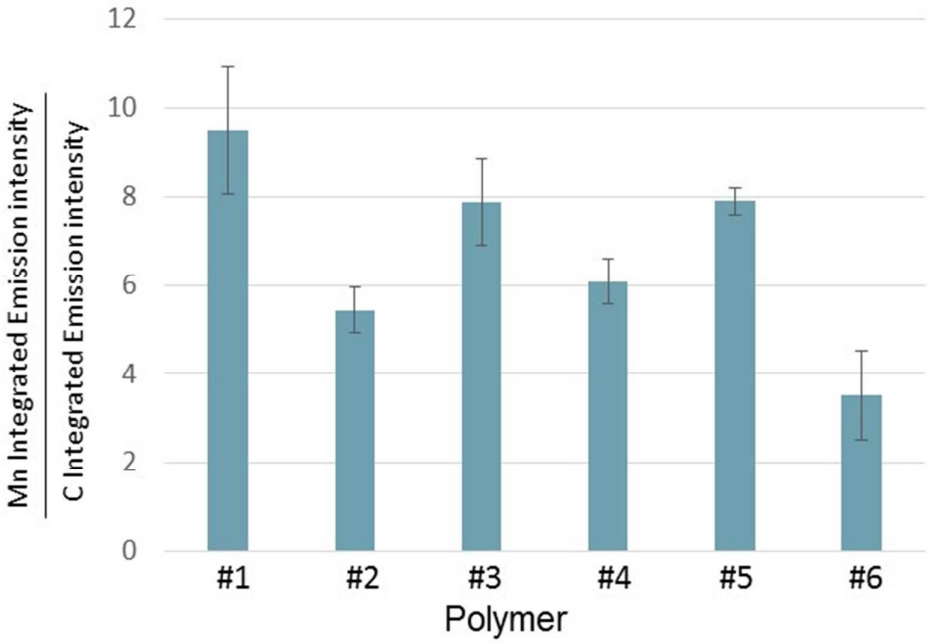

(a)

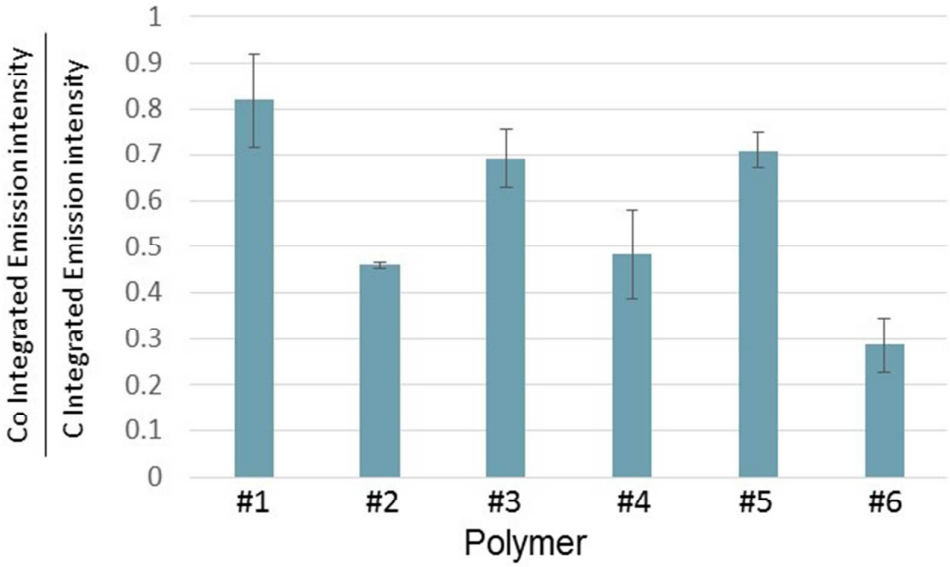

(b)

Figure 6. ICP-OES integrated emission intensity normalized to that obtained for carbon for the residues on six different polymers. (a) Manganese; (b) cobalt. Analytes concentration: 20 μg mL^{-1}.

View Article Online
DOI: 10.1039/C8JA00055G

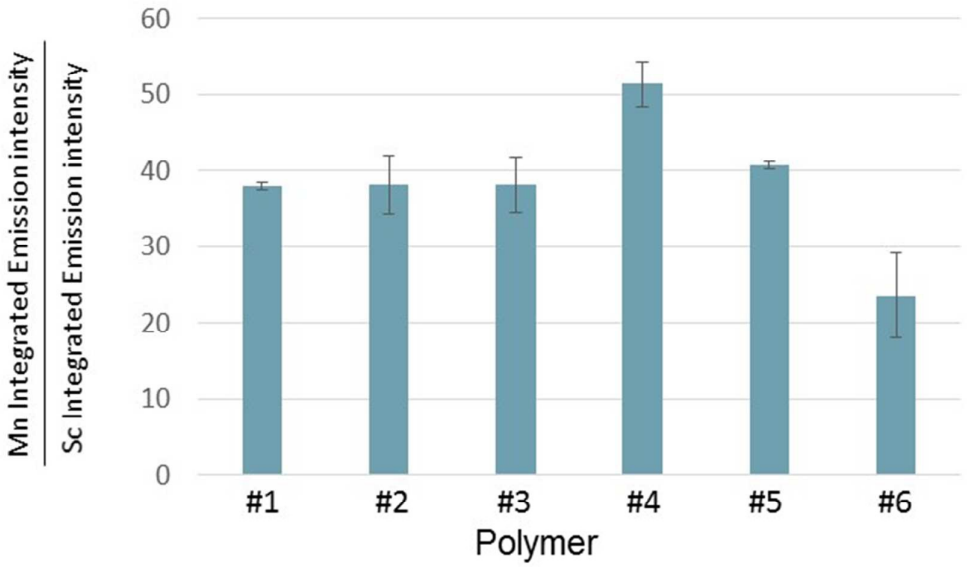

(a)

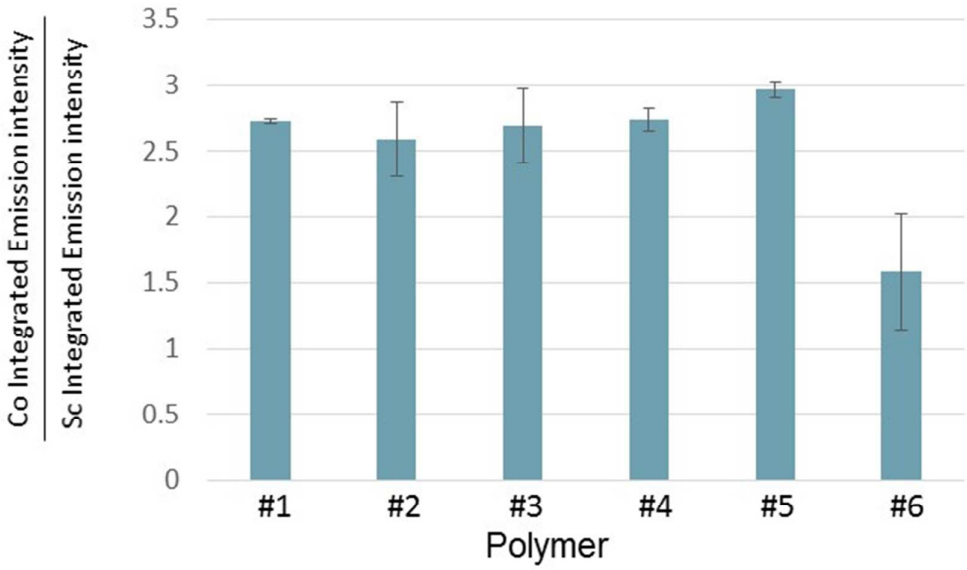

(b)

View Article Online
DOI: 10.1039/C8JA00055G

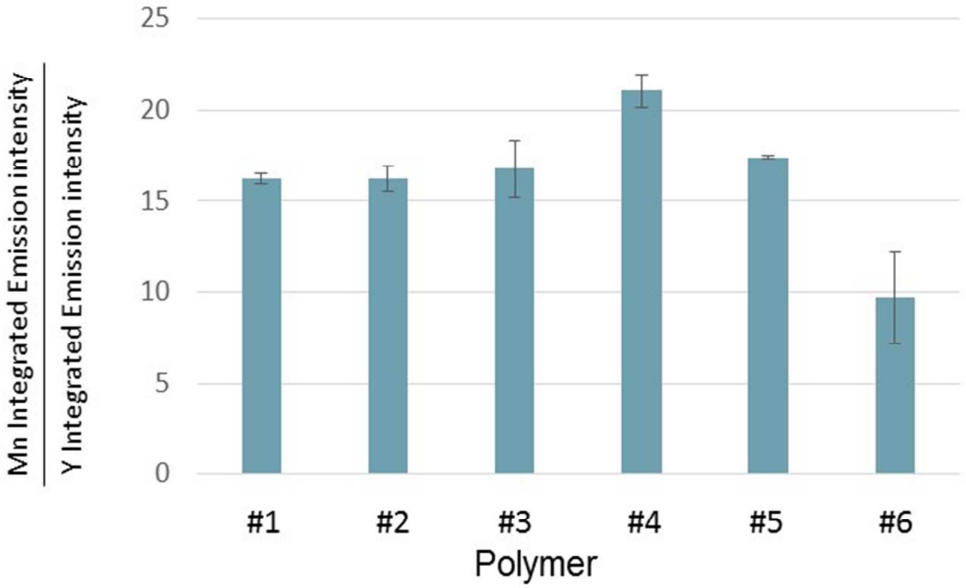

(c)

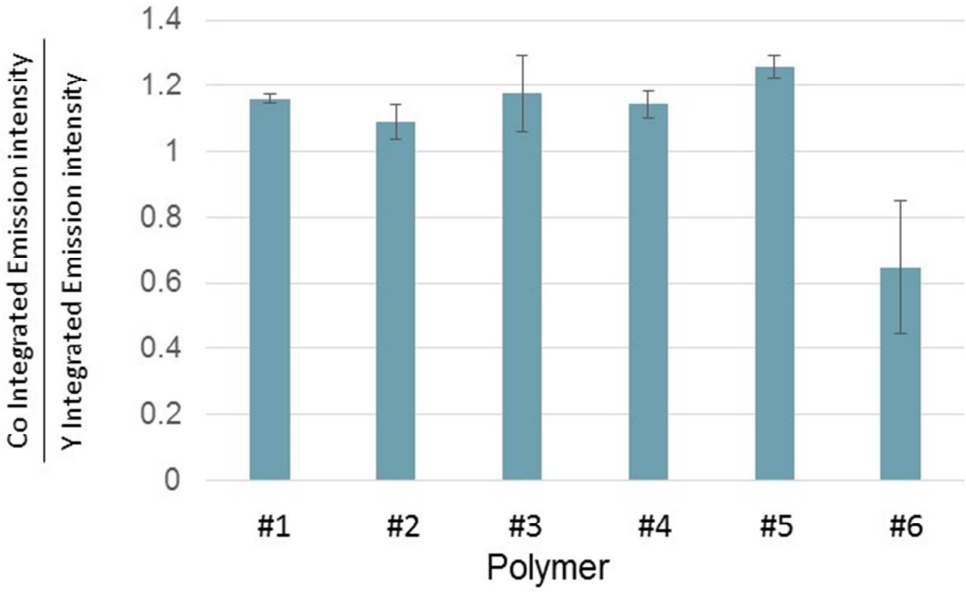

(d)

Figure 7. ICP-OES integrated emission intensity normalized to that obtained for scandium and yttrium as internal standards for the residues on six different polymers. (a) Manganese using scandium as IS; (b) cobalt using scandium as IS; (c)

View Article Online
DOI: 10.1039/C8JA00055G

manganese using yttrium as IS; (d) cobalt using yttrium as IS. Analytes concentration: 20 μg mL^{-1}.